



Local Delivery of Nimustine Hydrochloride against Brain Tumors: Basic Characterization Study

Xiaodong Shao,¹ Ryuta Saito,^{1,2} Aya Sato,¹ Saori Okuno,¹ Daisuke Saigusa,^{3,4,5} Ritsumi Saito,^{4,5} Akira Uruno,^{4,5} Yoshinari Osada,¹ Masayuki Kanamori¹ and Teiji Tominaga¹

¹Department of Neurosurgery, Tohoku University Graduate School of Medicine, Sendai, Miyagi, Japan

²Department of Neurosurgery, Nagoya University Graduate School of Medicine, Nagoya, Aichi, Japan

³Faculty of Pharma-Science, Teikyo University, Tokyo, Japan

⁴Department of Medical Biochemistry, Tohoku University Graduate School of Medicine, Sendai, Miyagi, Japan

⁵Department of Integrative Genomics, Tohoku Medical Megabank Organization, Tohoku University, Sendai, Miyagi, Japan

Convection-enhanced delivery (CED) delivers agents directly into tumors and the surrounding parenchyma. Although a promising concept, clinical applications are often hampered by insufficient treatment efficacy. Toward developing an effective CED-based strategy for delivering drugs with proven clinical efficacy, we performed a basic characterization study to explore the locally delivered characteristics of the water soluble nitrosourea nimustine hydrochloride (ACNU). First, ACNU distribution after CED in rodent brain was studied using mass spectrometry imaging. Clearance of ¹⁴C-labeled ACNU after CED in striatum was also studied. ACNU was robustly distributed in rodent brain similar to the distribution of the hydrophilic dye Evans blue after CED, and locally delivered ACNU was observed for over 24 h at the delivery site. Subsequently, to investigate the potential of ACNU to induce an immunostimulative microenvironment, Fas and transforming growth factor- β 1 (TGF- β 1) was assessed *in vitro*. We found that ACNU significantly inhibited TGF- β 1 secretion and reduced Fas expression. Further, after CED of ACNU in 9L-derived intracranial tumors, the infiltration of CD4/CD8 lymphocytes in tumors was evaluated by immunofluorescence. CED of ACNU in xenografted intracranial tumors induced tumor infiltration of CD4/CD8 lymphocytes. ACNU has a robust distribution in rodent brain by CED, and delayed clearance of the drug was observed at the local infusion site. Further, local delivery of ACNU affects the tumor microenvironment and induces immune cell migration in tumor. These characteristics make ACNU a promising agent for CED.

Keywords: convection-enhanced delivery; glioma; immunostimulation; nimustine hydrochloride; pharmacokinetics
Tohoku J. Exp. Med., 2023 November, 261 (3), 187-194.
doi: 10.1620/tjem.2023.J069

Introduction

Convection-enhanced delivery (CED) is a recently developed topical drug delivery designed to target lesioned areas in the central nervous system (CNS) (Bobo et al. 1994). It creates a continuous micropressure perfusion system at the microcatheter's infusion site and creates convection with pressure gradients in the surrounding brain tissue, thereby circumventing the blood-brain barrier (BBB) and interacting directly with the lesion (Brown et al. 2018). The

technique is widely used in basic research and in clinical trials of neurological disease treatment in recent years (Uckun et al. 2019; Tosi and Souweidane 2020; Merola et al. 2020).

In neuro-oncology, the application of CED to treat gliomas is appealing for several reasons: First, glioma is protected by the BBB so most chemotherapeutic drugs fail to achieve sufficient concentration within tumors without systemic side effects; second, glioma affects only the CNS, and metastasis outside the CNS is rare; and third, local recur-

Received May 17, 2023; revised and accepted August 7, 2023; J-STAGE Advance online publication August 25, 2023

Correspondence: Ryuta Saito, Department of Neurosurgery, Tohoku University Graduate School of Medicine, 1-1 Seiryomachi, Aoba-ku, Sendai, Miyagi 980-8574, Japan.

e-mail: ryuta@med.nagoya-u.ac.jp

©2023 Tohoku University Medical Press. This is an open-access article distributed under the terms of the Creative Commons Attribution-NonCommercial-NoDerivatives 4.0 International License (CC-BY-NC-ND 4.0). Anyone may download, reuse, copy, reprint, or distribute the article without modifications or adaptations for non-profit purposes if they cite the original authors and source properly.
<https://creativecommons.org/licenses/by-nc-nd/4.0/>

rence is the primary mode of recurrence in many cases (Zygogianni et al. 2018). Therefore, the concept of CED to achieve robust distribution within the targeted site with a high drug concentration is a promising strategy. However, although several large-scale clinical trials proved the safety and feasibility of this approach, its clinical efficacy still not confirmed (Laske et al. 1997; Kunwar et al. 2007).

Gliomas are resistant to cell death. Glia sharing the same cell of origin with gliomas including glial precursor cells usually do not turnover. We previously demonstrated that some glioma cells are resistant to interferon- β -induced apoptosis even though cell death pathway processes including caspase activation are observed (Saito et al. 2004). Glia and glioma may lack the mechanism of cell death (Fulda 2018), and accordingly, many studies testing molecular targeted agents against gliomas have failed (Touat et al. 2017). Among the large-scale studies testing CED against brain tumors (Laske et al. 1997; Rand et al. 2000; Kunwar et al. 2007), several sophisticated cytotoxic agents, such as TF-CRM107 (Laske et al. 1997), IL13-PE (Kunwar et al. 2007), and IL4-PE (Rand et al. 2000), have been tested. These agents are promising because they exert selective cytotoxicity against glioma cells; however, phase 3 trials reported unsatisfactory efficacies (Kunwar et al. 2007). Although a shortage of drug distribution was discussed as the main reason (Sampson et al. 2010), some reports considered that the problem lies with the agents themselves (Jarboe et al. 2007). These chimeric proteins exert cytotoxicity only when the glioma expresses the respective ligand for these agents (i.e., TF, IL-13, and IL-4 receptors).

In our development of an effective CED-based therapy, we used drugs that are clinically proven to be effective against gliomas, specifically temozolomide (Stupp et al. 2005), nitrosourea compounds (Stewart 2002), and bevacizumab (Vredenburgh et al. 2007). Among these agents, we focused on nitrosourea compounds due to their proven efficacy when applied locally, and their systemic use is limited by bone marrow toxicity. Of these compounds, nimustine hydrochloride (ACNU) was selected as it is the most hydrophilic, a characteristic which may be advantageous for local delivery by CED. In a previous study, we achieved an effective therapeutic effect by locally delivering ACNU (1 mg/mL) into the brain of rodents with intracranial tumors by CED, significantly prolonging rodent survival, and causing minimum toxic damage to the surrounding normal brain tissue (Sugiyama et al. 2007). Moreover, we recently demonstrated the possibility of this strategy in a clinical setting (Saito et al. 2011, 2020). However, we did not investigate ACNU distribution after CED in that study. Since infusate distribution is dependent on different factors, such as tissue affinity, charge, and molecular weight, it is an important issue for further development of this strategy (Saito et al. 2006). Moreover, considering its clinical application, the issue of distribution may be of greater importance as the human brain is much larger than rodent brain. In this study, we further investigated the basic characteristics of local

chemotherapy with ACNU against brain tumors.

Materials and Methods

Animals and cell lines

Male Fischer 344 rats with 6 to 8 weeks of age were purchased from Japan SLC, Inc. (Shizuoka, Japan). The protocols used in the animal studies were approved by the Institute for Animal Experimentation of the Tohoku University Graduate School of Medicine. Of the four human glioblastoma cell lines used in this study, U87, U251, and A172 were obtained from ECACC (Public Health England, London, UK), whereas T98 and the rat gliosarcoma cell line 9L were obtained from ATCC (Manassas, VA, USA). U87, U251, and T98 cells were cultured in Dulbecco's Modified Eagle Medium (DMEM) with 10% fetal bovine serum (FBS) and 100 U/mL penicillin/streptomycin, whereas A172 and 9L cells were cultured in DMEM with 10% FBS and 100 U/mL penicillin/streptomycin. All cells were maintained in a humidified incubator with 5% CO₂ at 37°C.

ACNU and Evans blue dye (EBD)

ACNU was purchased from Daiichi Sankyo Co., Ltd. (Tokyo, Japan) and diluted with 0.9% saline to a concentration of 1 mg/mL to treat 9L intracranial tumors. The hydrophilic dye EBD was purchased from Wako Co., Ltd. (Osaka, Japan) and diluted with 0.9% saline to a concentration of 2% v/v.

Biodistribution of ¹⁴C-labeled ACNU in rodent

To evaluate the biodistribution of ACNU after CED, ¹⁴C-labeled ACNU was synthesized by Sekisui Medical (Tokyo, Japan). The radiolabeled ACNU used in this study had a specific activity of 15 MBq/mg, MW of 309.15, and conversion factor of 0.938 (3.15/3.36). After a single CED of 0.02 mg ACNU/animal (0.0672 MBq in 20 μ L), systemic biodistribution was evaluated at different time points using autoradiography. For systemic quantitative autoradiography, whole-body sections of 30 μ m thickness were prepared by affixing each section to adhesive tape (810; 3M, Tokyo, Japan), followed by freeze drying, and covered with a 4- μ m-thick protective membrane (DIAFOIL, Mitsubishi Chemical, Tokyo, Japan) prior to exposure on a BAS SR2040 imaging plate (Fujifilm, Tokyo, Japan) for visualization.

ACNU distribution in rodent brain after CED

To evaluate ACNU distribution in rodent brain tissue, we locally delivered a mixture of ACNU with 2% EBD into normal rat brain by CED. Mass spectrometry imaging (MSI) at a spatial resolution of 75 μ m was used to visually analyze ACNU distribution (Supplemental File 1: detailed description in supplementary material and methods) (Urano et al. 2020). Spectra were acquired in the m/z range of 220–290 using a positive ionization mode and relative abundance of moxonidine hydrochloride (C₉H₁₄N₅OCl) [M+H]⁺ at m/z 244.10 in brain sections.

Brain tumor model

9L cells were used to generate intracranial tumors in rats. Cells were harvested in the logarithmic phase of cell growth, and a cell suspension of 5×10^7 cells/mL was prepared in cold phosphate-buffered saline (PBS). After anesthesia using isoflurane, rats were placed in a small-animal stereotactic frame (David Kopf Instruments, Los Angeles, CA, USA). Following exposure of the skull, a small dental drill was used to drill a hole on the skull surface (0.5 mm anterior and 3 mm lateral from the bregma). A 10 μ L Hamilton syringe (Hamilton Co., Bellefonte, PA, USA) with a 26-gauge needle was used to enter 4.5 mm from the brain surface to the striatum, and 2 μ L of PBS containing 1×10^5 9L cells was slowly injected over 3 min. The needle was withdrawn slowly after a 3-min wait, the burr hole was closed with bone wax, and the wound was sutured closed.

CED

Infusion was performed by CED as previously described (Sugiyama et al. 2007). Briefly, a reflux-free step-design infusion cannula connected to an oil-filled 1 mL syringe mounted on a BeeHive micro-infusion pump (Bioanalytical System, West Lafayette, IN, USA) was used to control the infusion rate. After deep anesthesia using isoflurane, rats were placed in a small-animal stereotactic frame (David Kopf Instruments), and a small dental drill was used to make a hole at the same location as the implant tumor. The depth of the needle was 4.5 mm from the brain surface, and the following ascending infusion rates were applied to achieve a 20 μ L total infusion volume: 0.2 μ L/min for 15 min, 0.5 μ L/min for 10 min, and 0.8 μ L/min for 15 min, followed by pump stoppage for 5 min before needle withdrawal.

Local delivery of ACNU into 9L intracranial tumors by CED

Six male Fischer 344 rats with 9L intracranial tumors were randomly divided into two groups 7 days after tumor cell implantation: CED of saline ($n = 3$) and CED of ACNU ($n = 3$). Seven days later, the rats were deeply anesthetized using isoflurane. The heart was exposed, and the left ventricle was perfused and fixed with cold saline and 4% paraformaldehyde in PBS. After removing the brain, it was fixed in 4% paraformaldehyde for 4 h at 4°C and then dehydrated in a gradient of 10%, 20%, and 30% sucrose. After complete fixation, brain tissue was embedded using Tissue-Tek OCT compound (Sakura Finetek, Tokyo, Japan) and stored at -80°C until use.

Enzyme-linked immunosorbent assay (ELISA)

To detect TGF- β 1 expression in 9L, U87, and U251 tumor cells after ACNU treatment, cells were cultured in 6-well plates (1×10^5 cells/well). Each tumor cell line had a control (saline, $n = 3$) and treatment (10 mM ACNU, $n = 3$) group. Supernatant was collected 24 h after treatment, and an ELISA kit (SB100B; R&D Systems, Minneapolis, MN, USA) was used to detect TGF- β 1 by measuring sam-

ple absorbance at 450 nm using a SPECTRA Max190 microplate reader (Molecular Device, San Jose, CA, USA).

Western blotting

U87, U251, T98, and A172 cells were cultured in 6-well plates (3×10^5 cells/well). Each tumor cell line had a control (saline, $n = 3$) and treatment (10 mM ACNU, $n = 3$) group. After 24-h treatment, whole-cell protein lysates were obtained for each tumor cell type using RIPA buffer (89901; Thermo Fisher Scientific, Waltham, MA, USA) containing protease and phosphatase inhibitors. Protein concentrations were determined using a BCA kit (23227; Thermo Fisher Scientific). Equal quantities of samples (15 μ g) were loaded on a 4-20% Mini-PROTEAN Gel (4561096; Bio-Rad, Hercules, CA, USA) and resolved by SDS-PAGE. The primary antibodies were a rabbit anti-Fas IgG polyclonal antibody (1:200 dilution; Sc-1023; Santa Cruz Biotechnology, Dallas, TX, USA) and a rabbit anti- β -actin IgG monoclonal antibody (1:20,000 dilution; 4970; Cell Signaling Technology, Danvers, MA, USA). After overnight incubation at 4°C, IgG Detector Solution v2 (T7122A; TaKaRa Bio, Kusatsu, Japan) was used as the secondary antibody and incubated at 20-22°C for 1 h. The antigen was detected by Pierce ECL Western Blotting Substrate (32106; Thermo Fisher Scientific), and a ChemiDoc MP imaging system (Bio-Rad) was used for image detection. Image Lab 6.0.1 (Bio-Rad) was used for quantitative analysis of protein gray value.

Immunofluorescence staining

To evaluate ACNU-induced immunity in 9L-derived intracranial tumors, we used immunofluorescence staining to detect CD4/CD8-positive T cells. Brain sections 8 μ m thick were cut using a Tissue-Tek Cryostat (Sakura Finetek) and blocked with 5% goat serum and 1% BSA with 0.1% Triton X-100 in PBS for 1 h at 20-22°C. Sections were incubated with a rabbit anti-rat CD4 IgG polyclonal antibody (1:200 dilution; NBP1-19371; NOVUS, Littleton, CO, USA) and mouse anti-rat CD8 α IgG1 monoclonal antibody (1:500 dilution; MCA48R; Bio-Rad) overnight at 4°C and then washed three times with PBS, followed by incubation with the secondary antibodies, a goat anti-rabbit IgG Alexa Fluor 488 (1:1,000 dilution; A-11034; Thermo Fisher Scientific) and a goat anti-mouse IgG Alexa Fluor 488 (1:1,000 dilution; A-11029; Thermo Fisher Scientific). DAPI (1:300 dilution; D1306; Invitrogen, Carlsbad, CA, USA) was used to stain nuclei by incubating for 1 h in the dark at 20-22°C. After three washes with PBS, samples were then covered with ProLong Diamond Antifade Mountant (P36961; Invitrogen) and detected using a DM4B imaging system (Leica, Wetzlar, Germany).

Statistical analysis

All *in vitro* experiments were independently performed three times, and the *in vivo* study used three rats in each group. Comparisons between groups were determined by

Student's t-test. All statistical analyses were performed with GraphPad Prism 8.4.3 (GraphPad Software Inc., San Diego, CA, USA). Significance was determined as $p < 0.05$.

Results

Biodistribution of ACNU in rodent brain after CED

ACNU (1 mg/mL) with 2% EBD was delivered locally into normal rat brain by CED. Since moxonidine hydrochloride ($C_9H_{14}N_5OCl$) is highly specific in the m/z 220-290 scan range, and it is a metabolite of ACNU, we selected $C_9H_{14}N_5OCl$ $[M+H]^+$ (m/z 244.10) as the detection molecule for MSI (Supplementary Fig. S1). Based on MSI analysis, ACNU was robustly distributed in brain tissue (Fig. 1A), in a pattern almost identical to the distribution of EBD after

local delivery by CED (Fig. 1B, C). Similar results were found in different sections of brain tissue (Fig. 1D-F).

Metabolism of ACNU in rodent after CED

Evaluation of ACNU metabolism was performed after local CED of ^{14}C -labeled ACNU in the brain of normal rats (Fig. 2A-E). Radiolabeled ACNU was detected in skin, bladder, and intestine of rats 5 min after local drug administration (Fig. 2A), which persisted for 8 h (Fig. 2D); no signal was detected at 24 h with the exception of the delivery site, where a high signal of radiolabeled ACNU was found (Fig. 2E). These findings show that a small amount of locally delivered ACNU may be cleared by intestinal and bladder metabolism in a short period of time, while a high concentration remains for a longer period at the local deliv-

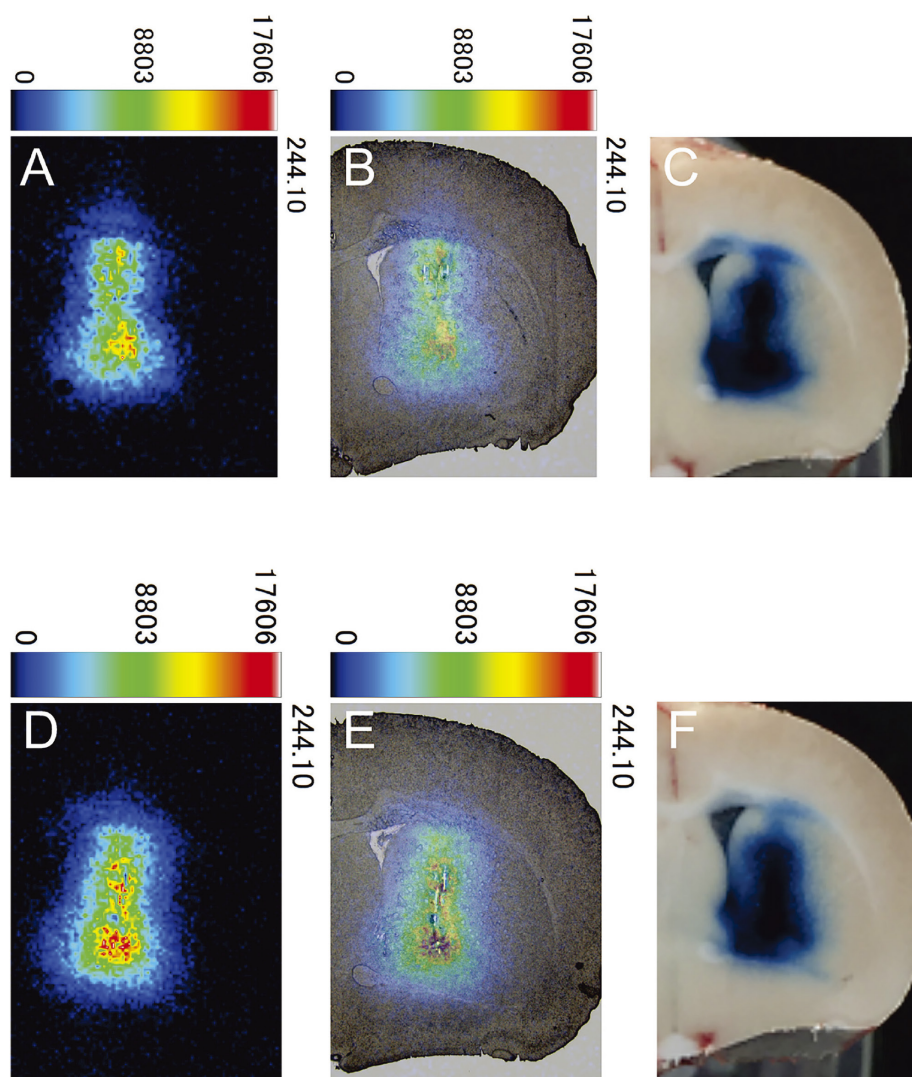


Fig. 1. Evaluation of ACNU distribution in rodent after CED.

All MSI data was collected at a spatial resolution of $75 \mu m$. (A) and (D) Distribution of the ACNU metabolite $C_9H_{14}N_5OCl$ $[M+H]^+$ in brain tissue after CED. (C) and (F) EBD distribution on sections at the same level as A. (B) and (E) Fusion of images (A)/(D) and (C)/(F). (A-C) and (D-F) Respective distribution of ACNU and EBD on the same sections at different brain areas; $80 \mu m$ interval between (A-C) and (D-F).

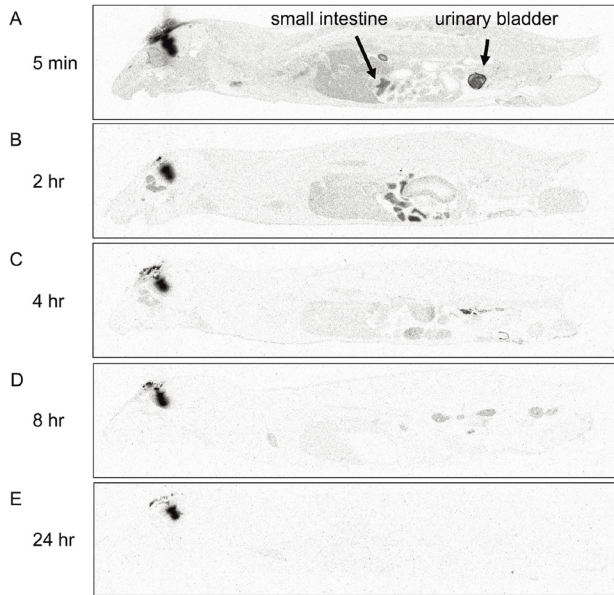


Fig. 2. Metabolism of ^{14}C -labeled ACNU in normal rats after local delivery by CED. Images obtained (A) 5 min, (B) 2 h, (C) 4 h, (D) 8 h, and (E) 24 h after CED.

ery area.

ACNU-induced changes to tumor microenvironment after CED

Fas immunoreactivity was evaluated *in vitro* in cells from tumor cell lines after ACNU treatment by western blot using whole-cell lysates 24 h after treatment. Compared with the respective control group, FAS immunoreactivity in U87, U251, T98, and A172 tumor cells treated with 10 mM ACNU was significantly decreased (Fig. 3A, B). TGF- β 1 secretion before and after ACNU administration was then evaluated in 9L, U87, and U251 cells. Compared with untreated cells, we found significant inhibition of TGF- β 1 secretion in cells from all three cell lines treated with 10 mM ACNU (Fig. 3C).

In vivo observation of ACNU-induced immunity after CED

Infiltration of CD4/CD8-positive T cells after ACNU treatment in our *in vivo* rodent brain tumor model was evaluated. Each rat locally received either saline (control group, $n = 3$) or ACNU (treatment group, $n = 3$) by CED 7 days after 9L intracranial tumor establishment. Brain sections were obtained 7 days after CED, and infiltration levels of CD4/CD8-positive T cells in tumor sites were detected and analyzed by immunofluorescence staining with anti-CD4 and anti-CD8 antibodies (Fig. 4A, green). We found that infiltration of CD4/CD8-positive T cells in the ACNU-treated group was significantly higher than that in the saline-treated control group (Fig. 4B, C; Supplementary Fig. S2), indicating that CED of ACNU-induced infiltration of immune cells *in vivo*.

Discussion

From a pharmacokinetics perspective, direct local delivery may be the best administration method for ACNU for several reasons. First, cytotoxic efficacy of ACNU is concentration dependent rather than duration of exposure (Newton 2006), and dose-limiting toxicity of ACNU is myelosuppression when delivered systemically (Shibui et al. 2013). We previously obtained indirect evidence of ACNU distribution after CED by co-infusing ACNU with EBD in intact non-human primate brain and evaluating ACNU content in brain tissue obtained immediately after infusion (Sugiyama et al. 2012). In this study, to directly prove the distribution, we used a pharmacokinetic method for the first time to visualize ACNU distribution after local delivery in normal rodent brain tissue. After infusion of ACNU with EBD, the MSI analysis was used to detect ACNU distribution, and we observed that ACNU had practically the same good distribution range as the hydrophilic dye EBD after local CED (Fig. 1). This finding concurs with our previous observation that local ACNU toxicity is concentration dependent rather than dose dependent as the local toxicity of drugs that fail to distribute becomes dose dependent (Zhang et al. 2014). Moreover, we analyzed ACNU metabolism *in vivo* using ^{14}C -labeled ACNU. ACNU was detected in the skin, digestive tract, and bladder of rats at 5 min, 2 h, 4 h, and 8 h after local delivery (Fig. 2A–D), essentially disappearing after 24 h (Fig. 2E). In intracerebral locally delivered areas, a sustained high signal of radiolabeled ACNU was detected until at least 24 h after administration (Fig. 2A–E). These results demonstrate that the hydrophilic drug ACNU not only has a robust distribution similar to EBD, but it also remains at the local infusion site for a prolonged duration. Some drug leaked into the systemic circulation at the very early phase of infusion; however, it was readily metabolized and excreted through the intestine and bladder in short order, reducing the risk of drug-related toxicity to other tissues and organs. These characteristics of robust distribution and delayed clearance after CED show that ACNU is a promising agent for CED in terms of pharmacokinetics.

We also previously demonstrated that local CED of ACNU transiently disrupted BBB integrity, thereby enabling systemic delivery of chemotherapeutic agents (Nakamura et al. 2011). Based on this observation and reports of immunostimulation after cytotoxic chemotherapy against various cancers (Shurin et al. 2012), we examined the effects of ACNU on tumor microenvironment *in vitro* and immune cell infiltration in tumors after CED. Fas immunoreactivity was determined in cells from four glioma cell lines (U87, U251, T98, and A172) before and after ACNU treatment. We found increased levels of Fas in ACNU-treated cells from all four glioma cell lines and that Fas immunoreactivity significantly decreased 24 h after ACNU treatment (Fig. 3A, B). Fas and FasL are critical survival factors for cancer cells that protect and promote

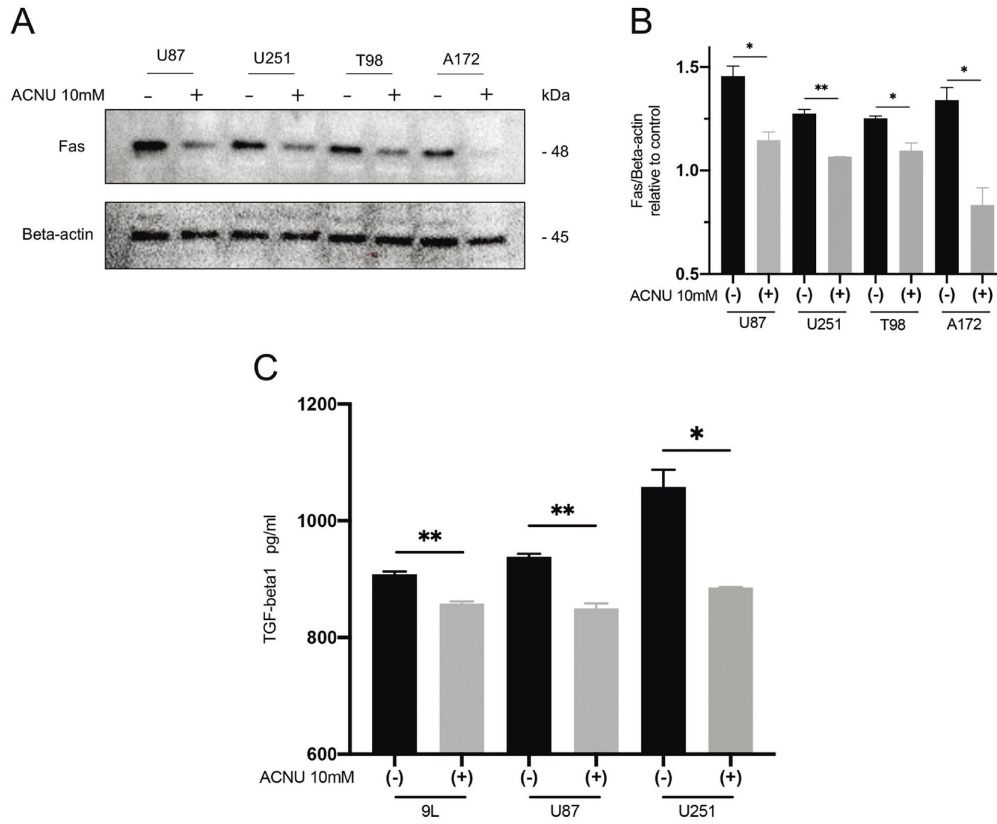


Fig. 3. ACNU reduced pFas expression and secretion of TGF- β 1 in cells from glioma cell lines *in vitro*. (A) Each cell line was treated with saline or 10 mM ACNU. Cells were harvested 24 h after treatment and pFas was detected by western blot. Compared with the saline-treated control group, pFas immunoreactivity in ACNU-treated cells was significantly decreased. β -Actin was used as an internal control. (B) Immunoreactivity for pFas was quantitatively analyzed. Bars indicate mean \pm standard deviation (SD). * $p < 0.05$, ** $p < 0.01$. (C) Cells from each tumor cell line were treated with saline (control group) or 10 mM ACNU (treatment group). After 24 h, the supernatant was collected and ELISA was performed to measure TGF- β 1. Compared with controls, the amount of secreted TGF- β 1 by ACNU-treated cells from each tumor cell line was significantly decreased. Bars indicate mean \pm SD. * $p < 0.05$, ** $p < 0.01$.

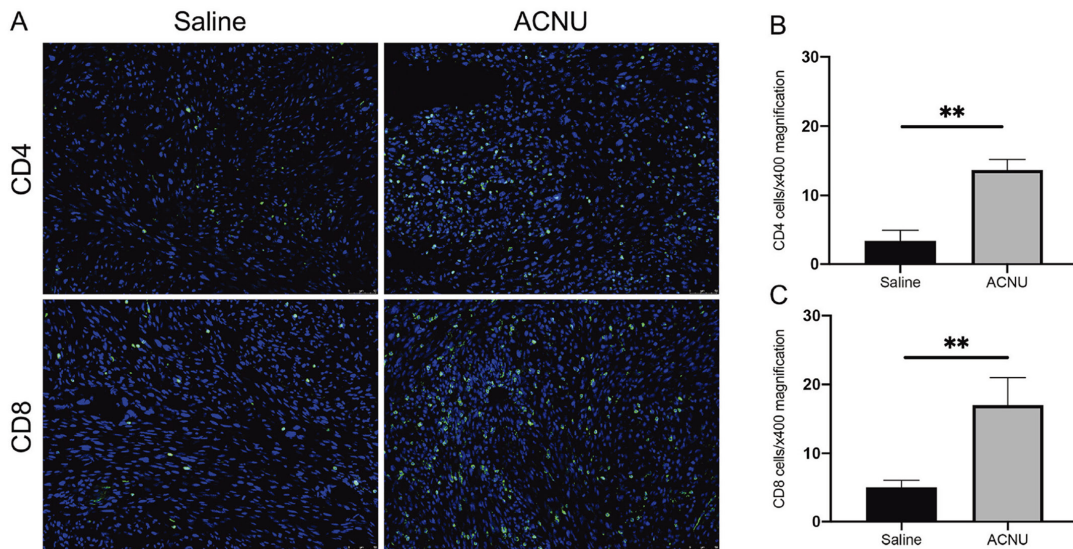


Fig. 4. Immune stimulation by local delivery of ACNU in a rodent 9L tumor model. (A) Immunofluorescence of rat CD4/CD8-positive T cells (green) in 9L tumors was performed using brains harvested 7 days after treatment. Nuclei were counterstained with DAPI (blue). Scale bars = 50 μ m. (B) and (C) The number of cells positively stained for CD4 and CD8 was counted under $\times 400$ magnification. Bars indicate mean \pm SD. ** $p < 0.01$.

cancer stem cells (Ceppi et al. 2014). Further, inhibiting or eliminating FasL, rather than augmenting it, may be beneficial for cancer therapy either alone or in combination with standard chemotherapy or immune therapy (Peter et al. 2015). ACNU also significantly inhibits secretion of TGF- β 1 in 9L, U87, and U251 cells (Fig. 3C). As a member of the TGF- β family of proteins, TGF- β 1 plays an important role in promoting differentiation and invasion of tumor cells (Eichhorn et al. 2012). TGF- β 1 also promotes activation of suppressive T cells, and TGF- β 1 secreted by suppressive T cells can further inhibit T-cell proliferation, thereby promoting immune escape of tumor cells (Platten et al. 2001). As both findings raise the possibility that ACNU can alter the immunosuppressive microenvironment, immune cell infiltration was examined using a 9L intracranial tumor model. After local delivery of ACNU into tumors by CED, significantly higher infiltration of CD4/CD8-positive T cells was observed relative to controls (Fig. 4).

In summary, we visually show for the first time ACNU distribution in rodent brain and its metabolism *in vivo* using a pharmacokinetic method. Transient disruption of the BBB and changes in tumor microenvironment may allow greater intratumoral infiltration of immune cells after CED of ACNU. These findings confirm the potential of ACNU for intratumoral delivery.

Acknowledgments

This research was supported in part by JSPS KAKENHI Grant Numbers JP21H03039, JP20K21641. We would like to thank Enago (<https://www.enago.jp>) for the English language review.

Conflict of Interest

The authors declare no conflict of interest.

References

- Bobo, R.H., Laske, D.W., Akbasak, A., Morrison, P.F., Dedrick, R.L. & Oldfield, E.H. (1994) Convection-enhanced delivery of macromolecules in the brain. *Proc. Natl. Acad. Sci. U. S. A.*, **91**, 2076-2080.
- Brown, C.B., Jacobs, S., Johnson, M.P., Southerland, C. & Threatt, S. (2018) Convection-enhanced delivery in the treatment of glioblastoma. *Semin. Oncol. Nurs.*, **34**, 494-500.
- Ceppi, P., Hadji, A., Kohlhapp, F.J., Pattanayak, A., Hau, A., Liu, X., Liu, H., Murmann, A.E. & Peter, M.E. (2014) CD95 and CD95L promote and protect cancer stem cells. *Nat. Commun.*, **5**, 5238.
- Eichhorn, P.J., Rodon, L., Gonzalez-Junca, A., Dirac, A., Gili, M., Martinez-Saez, E., Aura, C., Barba, I., Peg, V., Prat, A., Cuartas, I., Jimenez, J., Garcia-Dorado, D., Sahuquillo, J., Bernards, R., et al. (2012) USP15 stabilizes TGF-beta receptor I and promotes oncogenesis through the activation of TGF-beta signaling in glioblastoma. *Nat. Med.*, **18**, 429-435.
- Fulda, S. (2018) Cell death-based treatment of glioblastoma. *Cell Death Dis.*, **9**, 121.
- Jarboe, J.S., Johnson, K.R., Choi, Y., Lonser, R.R. & Park, J.K. (2007) Expression of interleukin-13 receptor alpha2 in glioblastoma multiforme: implications for targeted therapies. *Cancer Res.*, **67**, 7983-7986.
- Kunwar, S., Prados, M.D., Chang, S.M., Berger, M.S., Lang, F.F., Piepmeyer, J.M., Sampson, J.H., Ram, Z., Gutin, P.H., Gibbons, R.D., Aldape, K.D., Croteau, D.J., Sherman, J.W. & Puri, R.K.; Cintredekin Besudotox Intraparenchymal Study Group (2007) Direct intracerebral delivery of cintredekin besudotox (IL13-PE38QQR) in recurrent malignant glioma: a report by the Cintredekin Besudotox Intraparenchymal Study Group. *J. Clin. Oncol.*, **25**, 837-844.
- Laske, D.W., Youle, R.J. & Oldfield, E.H. (1997) Tumor regression with regional distribution of the targeted toxin TF-CRM107 in patients with malignant brain tumors. *Nat. Med.*, **3**, 1362-1368.
- Merola, A., Van Laar, A., Lonser, R. & Bankiewicz, K. (2020) Gene therapy for Parkinson's disease: contemporary practice and emerging concepts. *Expert Rev. Neurother.*, **20**, 577-590.
- Nakamura, T., Saito, R., Sugiyama, S., Sonoda, Y., Kumabe, T. & Tominaga, T. (2011) Local convection-enhanced delivery of chemotherapeutic agent transiently opens blood-brain barrier and improves efficacy of systemic chemotherapy in intracranial xenograft tumor model. *Cancer Lett.*, **310**, 77-83.
- Newton, H.B. (2006) CHAPTER 2 - Clinical Pharmacology of Brain Tumor Chemotherapy. In *Handbook of Brain Tumor Chemotherapy*, edited by Newton, H.B. Academic Press, San Diego, CA, pp. 21-43.
- Peter, M.E., Hadji, A., Murmann, A.E., Brockway, S., Putzbach, W., Pattanayak, A. & Ceppi, P. (2015) The role of CD95 and CD95 ligand in cancer. *Cell Death Differ.*, **22**, 549-559.
- Platten, M., Wick, W. & Weller, M. (2001) Malignant glioma biology: role for TGF-beta in growth, motility, angiogenesis, and immune escape. *Microsc. Res. Tech.*, **52**, 401-410.
- Rand, R.W., Kreitman, R.J., Patronas, N., Varricchio, F., Pastan, I. & Puri, R.K. (2000) Intratumoral administration of recombinant circularly permuted interleukin-4-Pseudomonas exotoxin in patients with high-grade glioma. *Clin. Cancer Res.*, **6**, 2157-2165.
- Saito, R., Kanamori, M., Sonoda, Y., Yamashita, Y., Nagamatsu, K., Murata, T., Mugikura, S., Kumabe, T., Wembacher-Schroder, E., Thomson, R. & Tominaga, T. (2020) Phase I trial of convection-enhanced delivery of nimustine hydrochloride (ACNU) for brainstem recurrent glioma. *Neurooncol. Adv.*, **2**, vdaa033.
- Saito, R., Krauze, M.T., Noble, C.O., Tamas, M., Drummond, D.C., Kirpotin, D.B., Berger, M.S., Park, J.W. & Bankiewicz, K.S. (2006) Tissue affinity of the infusate affects the distribution volume during convection-enhanced delivery into rodent brains: implications for local drug delivery. *J. Neurosci. Methods*, **154**, 225-232.
- Saito, R., Mizuno, M., Hatano, M., Kumabe, T., Yoshimoto, T. & Yoshida, J. (2004) Two different mechanisms of apoptosis resistance observed in interferon-beta induced apoptosis of human glioma cells. *J. Neurooncol.*, **67**, 273-280.
- Saito, R., Sonoda, Y., Kumabe, T., Nagamatsu, K., Watanabe, M. & Tominaga, T. (2011) Regression of recurrent glioblastoma infiltrating the brainstem after convection-enhanced delivery of nimustine hydrochloride. *J. Neurosurg. Pediatr.*, **7**, 522-526.
- Sampson, J.H., Archer, G., Pedain, C., Wembacher-Schroder, E., Westphal, M., Kunwar, S., Vogelbaum, M.A., Coan, A., Herndon, J.E., Raghavan, R., Brady, M.L., Reardon, D.A., Friedman, A.H., Friedman, H.S., Rodriguez-Ponce, M.I., et al. (2010) Poor drug distribution as a possible explanation for the results of the PRECISE trial. *J. Neurosurg.*, **113**, 301-309.
- Shibui, S., Narita, Y., Mizusawa, J., Beppu, T., Ogasawara, K., Sawamura, Y., Kobayashi, H., Nishikawa, R., Mishima, K., Muragaki, Y., Maruyama, T., Kuratsu, J., Nakamura, H., Kochi, M., Minamida, Y., et al. (2013) Randomized trial of chemoradiotherapy and adjuvant chemotherapy with nimustine (ACNU) versus nimustine plus procarbazine for newly diagnosed anaplastic astrocytoma and glioblastoma (JCOG0305). *Cancer Chemother. Pharmacol.*, **71**, 511-521.
- Shurin, M.R., Naiditch, H., Gutkin, D.W., Umansky, V. & Shurin,

- G.V. (2012) ChemoImmunoModulation: immune regulation by the antineoplastic chemotherapeutic agents. *Curr. Med. Chem.*, **19**, 1792-1803.
- Stewart, L.A. (2002) Chemotherapy in adult high-grade glioma: a systematic review and meta-analysis of individual patient data from 12 randomised trials. *Lancet*, **359**, 1011-1018.
- Stupp, R., Mason, W.P., van den Bent, M.J., Weller, M., Fisher, B., Taphoorn, M.J., Belanger, K., Brandes, A.A., Marosi, C., Bogdahn, U., Curschmann, J., Janzer, R.C., Ludwin, S.K., Gorlia, T., Allgeier, A., et al. (2005) Radiotherapy plus concomitant and adjuvant temozolomide for glioblastoma. *N. Engl. J. Med.*, **352**, 987-996.
- Sugiyama, S., Saito, R., Nakamura, T., Yamashita, Y., Yokosawa, M., Sonoda, Y., Kumabe, T., Watanabe, M. & Tominaga, T. (2012) Safety and feasibility of convection-enhanced delivery of nimustine hydrochloride co-infused with free gadolinium for real-time monitoring in the primate brain. *Neurol. Res.*, **34**, 581-587.
- Sugiyama, S., Yamashita, Y., Kikuchi, T., Saito, R., Kumabe, T. & Tominaga, T. (2007) Safety and efficacy of convection-enhanced delivery of ACNU, a hydrophilic nitrosourea, in intracranial brain tumor models. *J. Neurooncol.*, **82**, 41-47.
- Tosi, U. & Souweidane, M. (2020) Convection enhanced delivery for diffuse intrinsic pontine glioma: review of a single institution experience. *Pharmaceutics*, **12**, 660.
- Touat, M., Idbaih, A., Sanson, M. & Ligon, K.L. (2017) Glioblastoma targeted therapy: updated approaches from recent biological insights. *Ann. Oncol.*, **28**, 1457-1472.
- Uckun, F.M., Qazi, S., Hwang, L. & Trieu, V.N. (2019) Recurrent or refractory high-grade gliomas treated by convection-enhanced delivery of a TGFbeta2-targeting RNA therapeutic: a post-hoc analysis with long-term follow-up. *Cancers (Basel)*, **11**, 1892.
- Urano, A., Matsumaru, D., Ryoke, R., Saito, R., Kadoguchi, S., Saigusa, D., Saito, T., Saido, T.C., Kawashima, R. & Yamamoto, M. (2020) Nrf2 suppresses oxidative stress and inflammation in App knock-in Alzheimer's disease model mice. *Mol. Cell. Biol.*, **40**, e00467-19.
- Vredenburgh, J.J., Desjardins, A., Herndon, J.E. 2nd, Marcello, J., Reardon, D.A., Quinn, J.A., Rich, J.N., Sathornsumetee, S., Gururangan, S., Sampson, J., Wagner, M., Bailey, L., Bigner, D.D., Friedman, A.H. & Friedman, H.S. (2007) Bevacizumab plus irinotecan in recurrent glioblastoma multiforme. *J. Clin. Oncol.*, **25**, 4722-4729.
- Zhang, R., Saito, R., Mano, Y., Kanamori, M., Sonoda, Y., Kumabe, T. & Tominaga, T. (2014) Concentration rather than dose defines the local brain toxicity of agents that are effectively distributed by convection-enhanced delivery. *J. Neurosci. Methods*, **222**, 131-137.
- Zygiogianni, A., Protopapa, M., Kougioumtzopoulou, A., Simopoulou, F., Nikoloudi, S. & Kouloulis, V. (2018) From imaging to biology of glioblastoma: new clinical oncology perspectives to the problem of local recurrence. *Clin. Transl. Oncol.*, **20**, 989-1003.

Supplementary Files

Please find supplementary file(s);
<https://doi.org/10.1620/tjem.2023.J069>